平成 29 年度学位申請論文

Modulation of immunological activity on macrophages induced by diazinon

（ダイアジノンが誘導するマクロファージの免疫修飾活性）

名古屋大学大学院医学系研究科
医療技術学専攻

（指導：川部　勤　教授）

小　笠　原　名　奈　子

Abstract

Diazinon is an organophosphorus (OP) insecticide and is widely used not only in agriculture but also homes and garden in Japan. Diazinon has been reported to increase TNF-α production in rat serum and brain, suggesting that it can modify the proinflammatory response. In this study, we investigated the effects of diazinon on macrophage functions, such as cytokine production, reactive oxygen species (ROS) generation, cyclooxygenase (COX)-2 and inducible nitric oxide synthase (iNOS) expressions, cell-surface molecule expressions, and phagocytosis in RAW264.7 cells. In RAW264.7 cells, diazinon induced the production of TNF-α and IL-6. Diazinon induced ROS generation and the expressions of COX-2, iNOS, and cell-surface molecules CD40, CD86, and MHC class II, but reduced phagocytic activity in RAW264.7 cells. ERK and p38, but not JNK and p65 were involved in diazinon-induced IL-6 expression in RAW264.7 cells. We also examined these proinflammatory responses in bone marrow-derived macrophages (BMDM) and bronchoalveolar lavage fluid (BALF) cells. These results suggested that diazinon can activate macrophages and enhance inflammatory responses.

ダイアジノンは有機リン系殺虫剤であり日本では農業だけでなく屋内や園芸にも広く使用されている。ラットの血清中および脳においてダイアジノンが TNF-α の産生を増強させることが報告されていることから、ダイアジノンが炎症反応を修飾する可能性が示唆される。本研究では、ダイアジノンが炎症性サイトカインの産生、活性酸素種 (ROS)の産生、シクロオキシゲナーゼ (COX)-2 および誘導型一酸化窒素合成酵素 (iNOS)の発現、細胞表面分子の発現および貪食能など、マクロファージの機能に及ぼす影響について RAW264.7 細胞を用いて検討した。RAW264.7 細胞においてダイアジノンは TNF-α および IL-6 の産生、ROS の産生、COX-2 および iNOS の発現、細胞表面分子（CD40、CD86、MHC class II）の発現を増強したが、貪食能は低下させた。また、RAW264.7 細胞においてダイアジノンが誘導する IL-6 の発現には JNK および p65 ではなく ERK および p38 が関与していた。さらに、骨髄由来マクロファージ (BMDM)およびマウス気管支肺胞洗浄液 (BALF)中の細胞を用いてこれらの炎症反応を検討した。

以上の結果より、ダイアジノンはマクロファージを活性化し、炎症反応を増強する可能性が示唆された。

Abbreviations: OP, Organophosphorus; AChE, acetyl-cholinesterase; ROS, reactive oxygen species; COX, cyclooxygenase; iNOS, inducible nitric oxide synthase; BALF, bronchoalveolar lavage fluid; HO, heme oxygenase; NF-κB, nuclear factor-kappa B; MAP kinase, mitogen-activated protein kinase; ERK, extracellular signal-regulated kinase; JNK, c-Jun N-terminal kinase

1. Introduction

Organophosphorus (OP) insecticides are widely used in agriculture and have broad-spectrum insecticidal activity. The main mechanism of OP insecticide toxicity is the inhibition of acetyl-cholinesterase (AChE) activity by overstimulation of nicotinic and muscarinic receptors (Flaskos, 2012). OP insecticides are also toxic to humans, and exposure of OP insecticides by inhalation results in nausea, dizziness, muscular dysfunction, respiratory failure, and pulmonary edema (Banerjee et al., 2012). Diazinon is an OP insecticide and used not only in agriculture, but also for home gardening and indoor pest control (Win-Shwe et al., 2013). Although it has been prohibited for residential use in the U.S. since 2004 due to its toxicity, there is still a large quantity of diazinon on the market in Japan (Pizzurro et al., 2014). Diazinon has been reported to increase TNF-α production in rat serum and brain (Ahmed et al., 2013; Hariri et al., 2010). It also causes toxic effects on blood cells, spleen, thymus, and lymph nodes in mice, suggesting that it can modify the immune system (Handy et al., 2002). Although various alternative molecular targets and mechanisms of OP insecticides have been reported (Banks and Lein, 2012; Terry, 2012), less is known about the target cells or target molecules of diazinon that affect the immune system.

Macrophages are widely distributed and play an indispensable role in homeostasis, and innate and adaptive immunity. Macrophages are involved in various immune function, such as phagocytosis, enzyme liberation, free radical generation, antigen presentation, and as release of inflammatory mediators (Gordon, 2003). Activated macrophages rapidly induce the expression of genes responsible for the synthesis of reactive oxygen and nitrogen species and bioactive lipids derived from arachidonic acid. A recent study has shown that parathion, an OP, activates macrophages to release TNF-α and induces airway hyperreactivity (Proskocil et al., 2013). Diazinon has also been reported to induce bronchoconstriction after subcutaneous injection (Lein and Fryer,

2005). Since diazinon enters the body via skin contact, feeding, and inhalation, and macrophages are abundant in these areas, we hypothesized that diazinon could affect the immune system by changing macrophage functions.

In this study, we investigated the effects of diazinon on macrophage functions, such as cytokine production, reactive oxygen species (ROS) generation, cyclooxygenase (COX)-2 and inducible nitric oxide synthase (iNOS) expressions, cell-surface molecule expressions, and phagocytosis in macrophages.

2. Materials and methods

2.1. Reagents

Diazinon, PD98059, and SB202190 were obtained from Sigma (St. Louis, MO). Tetrazolium salt WST-1 (4-[3-(4-Iodophenyl)-2-(4-nitrophenyl)-2H-5-tetrazolio-1,3-benzene disulfonate]) was from Roche (Basel, Switzerland). 2',7'-dichlorodihydrofluorescein diacetate (H_2DCF-DA) was from Molecular Probes, Inc. (Eugene, OR).

2.2. Animals

Wild-type (WT) C57BL/6 mice were purchased from SLC (Shizuoka, Japan). Animals were maintained in a temperature (22-24°C), humidity (55±5%), and light (12 h light-dark cycle; lights on at 8:00) regulated room with access to food and water *ad libitum*. Animal experiments were approved by the Animal Experiment Committee of Nagoya University Graduate School of Medicine. All procedures were performed in accordance with the Guidelines for Animal Experimentation of Nagoya University.

2.3. Collection of bronchoalveolar lavage fluid (BALF) cells

BALF was collected as previously described (Takashima et al., 2014; Yasui et al., 2015). Briefly, mice were exsanguinated by aortic perforation under pentobarbital anesthetization. The trachea was cannulated, and the lungs were lavaged six times with PBS (0.5 ml each time). Collected BALF cells were centrifuged at 1200 rpm for 3 min, and pelleted cells were then re-suspended in RPMI1640 medium supplemented with 100 U/ml penicillin, 100 μg/ml streptomycin, 0.25 μg/ml amphotericin B, MEM non-essential amino acids, 1 mM sodium pyruvate, 50 μM 2-mercaptoethanol, and 10% fetal bovine serum (FBS). More than 95% of BALF cells were macrophages as assessed by May-Grünwald and Giemsa staining.

2.4. Generation of bone marrow-derived macrophages (BMDM)

Bone marrow cells were isolated from C57BL/6 mice and cultured in RMPI1640 medium with 100 U/ml penicillin, 100 μg/ml streptomycin, 0.25 μg/ml amphotericin B, MEM non-essential amino acids, 1 mM sodium pyruvate, 50 μM 2-mercaptoethanol, and 10% FBS containing 10 ng/ml granulocyte macrophage colony-stimulating factor (GM-CSF) (PeproTech, Rocky Hill, NJ) for 7 days. GM-CSF was removed the day before experiments. The differentiation into macrophages were determined by the expression levels of CD11b.

2.5. Cell culture

The murine monocyte/macrophage cell line RAW264.7 was purchased from the American Type Culture Collection (Manassas, VA, USA). RAW264.7 cells were maintained in RPMI1640 medium containing 100 U/ml penicillin, 100 μg/ml streptomycin, 0.25 μg/ml amphotericin B, 1 mM sodium pyruvate, MEM non-essential amino acids, and 10% FBS. Cells were grown under standard conditions in a humidified incubator at 37ºC and 5% CO_2.

2.6. Cell viability assay

RAW264.7 cells were incubated in a 96-well plate with or without various concentrations of diazinon for 24 h. A colorimetric assay was performed based on the cleavage of the tetrazolium salt WST-1 (4-[3-(4-Iodophenyl)-2-(4-nitrophenyl)-2H-5-tetrazolio]-1,3-benzene disulfonate) (Roche, Basel, Switzerland) by mitochondrial dehydrogenases in viable cells. WST-1 was added to each well, and cells were incubated for 1 h. The plate was read at a wavelength of 450 nm with a reference at 650 nm with a microplate reader (Bio-Rad Laboratories, Hercules, CA).

2.7. Reverse transcription-polymerase chain reaction (RT-PCR), quantitative real-time PCR

Total RNA was isolated using ISOGEN II (Nippon Gene, Toyama, Japan) and reverse-transcribed to cDNA using PrimeScript RT MasterMix (Takara Bio, Otsu, Japan). Quantitative real-time PCR was performed on the Thermal Cycler Dice Real Time System II (TaKaRa Bio, Otsu, Japan) as previously described (Takashima et al., 2014). Primers and probes for *Tnfa*, *Il6*, *Cox2*, *Nos2*, and *Gapdh* were obtained from Nippon EGT (Toyama, Japan). Transcripts of *Gapdh*, as a house keeping gene, were quantified as an endogenous reference RNA to normalize each sample. Relative quantities of expression were estimated by the standard curve method. The results were normalized as relative expression in which the average values of *Tnfa*, *Il6*, *Cox2*, or *Nos2* were divided by the average value of *Gapdh*. The ratio was calculated by dividing the normalized values of stimulated cells by the values in control cells.

2.8. Enzyme-linked immunosorbent assay (ELISA)

Cells were cultured with diazinon for 24 h, and the supernatant was collected for ELISA analysis. The cytokine productions of TNF-α and IL-6 were assayed using a murine ELISA development kit (Affymetrix, Santa Clara, CA).

2.9. Measurement of intracellular ROS

Levels of intracellular ROS were assessed using 2',7'-dichlorodihydrofluorescein diacetate (H_2DCF-DA) (Thermo Fisher Scientific, San Jose, CA). Briefly, cells were incubated with 50 μM H_2DCF-DA for 15 min and then treated with 600 μM diazinon for 15 min. Cells were subsequently washed with PBS and detached with trypsin. After centrifugation, the cell pellet was resuspended in 400 μl PBS. Intracellular ROS

production was detected using a FACSCalibur flow cytometer (Becton Dickinson, Franklin Lakes, NJ) and quantified using FlowJo software program (Flowjo LLC, Ashland, OR).

2.10. Western blotting

Twenty μg of protein was subjected to SDS-PAGE using a 12% separation gel and transferred to a polyvinylidene difluoride membrane (Millipore, Billerica, MA). The membrane was blocked by incubation (1 h at room temperature) with 2% skim milk or 2% bovine serum albumin. The membrane was then incubated (overnight at 4°C) with primary antibodies. Subsequently, the membrane was incubated (1 h at room temperature) with either anti-rabbit IgG or anti-mouse IgG antibodies conjugated with HRP. The specific protein bands on the membrane were visualized using the Enhanced Chemiluminescence Kit (Millipore) according to the recommendations of the manufacturer. The expression levels were quantified using Scion image software (Scion Corporation, Frederick, MD).

2.11. Flow cytometric analysis of cell-surface molecule expression

After stimulation with diazinon for 25 h, cells were incubated with biotin or fluorescent-labeled antibodies (anti-CD40, CD80, CD86, CD11b, and MHC class II) (Becton Dickinson) at room temperature for 20 min. Biotin conjugates were visualized with PE-Cy7-streptavidin (Becton Dickinson). The expression of cell-surface molecules was analyzed by a FACSCalibur flow cytometer or FACSCanto II flow cytometer (Becton Dickinson) and quantified using FlowJo software program.

2.12. Phagocytosis assay

Phagocytosis assays were performed as described previously (Shibasaki et al., 2009).

After stimulation with diazinon for 20 h, cells were incubated with FITC-labeled latex beads (Polysciences, Warrington, PA) in culture medium for 2 h at 37ºC, and washed gently with 0.025% Tween 20 in PBS. The stained cells were evaluated on a FACSCalibur flow cytometer or FACSCanto II flow cytometer and quantified using FlowJo software program.

2.13. Statistical analysis

Statistical comparisons among the groups were assessed by one-way analysis of variance (ANOVA). When F ratios were significant ($p<0.05$), Scheffe's *post hoc* tests between two groups were done, and $p<0.05$ were considered statistically significant *post hoc* differences. Statistical analyses were performed with StatView (Abacus concept Inc., Gloucestershire, UK).

3. Results

3.1. Effects of diazinon on cell viability of RAW264.7 cells

To determine the optimal (non-toxic) concentration of diazinon for investigation, we checked the effect of diazinon on cell viability (**Fig. 1A**). RAW264.7 cells were incubated with various concentrations of diazinon (0-600 μM) for 24 h and subjected to the WST-1 assay. Based on the results, we used diazinon at or below concentrations of 600 μM for the following experiments.

3.2. Diazinon induced expression and production of proinflammatory cytokines in RAW264.7 cells

To investigate whether diazinon could affect cytokine production by macrophages, we evaluated the expression and production of TNF-α and IL-6 as proinflammatory cytokines. RAW 264.7 cells were stimulated with diazinon 600 μM for 1 or 4 h, and the levels of TNF-α and IL-6 mRNA expression were examined by quantitative real-time PCR (**Fig. 1B)**. Stimulation with diazinon led to a significant increase in the levels of TNF-α and IL-6 mRNA expressions in RAW264.7 cells. The expression levels of each cytokine mRNA were increased up to 5.4-fold for TNF-α and 48.8-fold for IL-6 compared to the control. The effect of cytokine production in the culture supernatant after stimulation with diazinon was also examined by ELISA (**Fig. 1C**). Exposure to diazinon significantly induced the production of TNF-α (1963±253 pg/ml) and IL-6 (2.93±0.78 pg/ml) in RAW264.7 cells. These results suggest that diazinon can activate macrophages to produce cytokines.

3.3. Diazinon induced ROS generation and HO-1 expression in RAW264.7 cells

We next investigated diazinon-induced ROS generation in RAW264.7 cells. RAW264.7 cells were loaded for 15 min with 50 μM H_2DCF-DA, which interacts with

ROS, and then exposed to diazinon for 15 min. Generation of ROS was increased by diazinon compared to vehicle (DMSO)-treated control (**Fig. 2A**). Moreover, diazinon significantly induced the expression of heme oxygenase (HO)-1, an antioxidant enzyme induced by ROS (**Fig. 2B**). These results suggest that diazinon can cause oxidative stress to macrophages. Excessive ROS induce the expression of inflammatory mediators such as COX-2 and iNOS. We next examined the expressions of COX-2 and iNOS under stimulation with diazinon. RAW264.7 cells were stimulated with 600 μM diazinon for 4 h, and the levels of COX-2 and iNOS mRNA expressions were examined by quantitative real-time PCR. Both COX-2 and iNOS expression were increased after stimulation with diazinon (**Fig. 2C**).

3.4. Effects of diazinon on the expression of cell-surface molecules

When activated to become effector cells, macrophages change the pattern of cell-surface antigen expression. We next examined the expression levels of several cell-surface molecules, including CD40, CD80, CD86, and MHC class II as co-stimulatory molecules by flow cytometry. After stimulation with 600 μM diazinon for 25 h in RAW264.7 cells, the expression levels of CD40, CD86, and MHC class II, but not CD80, were significantly increased (**Fig. 3**).

3.5. Effects of diazinon on phagocytosis

To further assess the effects of diazinon on macrophages, we examined phagocytosis as a physiological functions of macrophages. After stimulation with diazinon for 20 h, phagocytic internalization of FITC-labeled latex beads by RAW264.7 cells were evaluated. Cells stimulated with diazinon showed remarkably decreased phagocytosis compared to controls (**Fig. 4**).

3.6. Effects of diazinon on phosphorylation of NF-κB and MAP kinase

The induction of proinflammatory cytokines, as well as other inflammatory mediators following macrophage activation induced by inflammatory stimuli, including LPS, are regulated by the transcription factor NF-κB. We investigated whether the effect of diazinon was mediated by NF-κB. RAW264.7 cells were treated with diazinon for 20 min, and the phosphorylation of p65, a subunit of NF-κB, as well as MAP kinases, including ERK, p38, and JNK, were evaluated by western blotting. Diazinon failed to induce phosphorylation of p65 (**Fig. 5A**). Moreover, diazinon induced phosphorylation of ERK and p38, but not JNK **(Fig. 5A)**. ERK inhibitor, PD98059 and p38 inhibitor, SB202190, significantly inhibited the induction of IL-6 mRNA expression **(Fig. 5B)**, suggesting that ERK- and p38-dependent signal pathway would exist to modulate macrophage activation induced by diazinon.

3.7. Effects of diazinon on the expression of cell-surface molecules and phagocytosis in BMDM

We next generated BMDM and further examined the expression levels of CD40, CD80, CD86, and MHC class II, and phagocytosis after exposure to diazinon. Bone marrow cells from C57BL/6 mice were isolated and cultured with GM-CSF for 7 days to differentiate into macrophages. Diazinon increased the expression levels of CD86 in BMDM whereas these levels were far lower than those of CD40, CD80, and MHC class II (**Fig. 6A**). BMDM had higher phagocytic activity in normal condition, and diazinon remarkably decreased its activity (**Fig. 6B**).

3.8. Effects of diazinon on cytokine expression in mouse BALF cells

To further investigate the effects of diazinon, we examined the activation of macrophages induced by diazinon under *ex vivo* conditions. Specifically, BALF cells

were isolated from C57BL/6 mice and stimulated with diazinon. We found that diazinon significantly induced the expression of TNF-α and IL-6 (**Fig. 7**). These results suggested that diazinon can activate macrophages under physiological conditions.

4. Discussion

In this study, we investigated the effects of diazinon on macrophage activation in RAW264.7 cells. Diazinon induced ROS generation and the expressions of TNF-α, IL-6, COX-2, iNOS, and cell-surface molecules, including CD40, CD86, and MHC class II. However, phagocytic activity in contrast was reduced in RAW264.7 cells.

The primary target of OP insecticides is AChE activity, responsible for hydrolyzing acetylcholine (Flaskos, 2012). It is unclear whether the activation of macrophages by diazinon was mediated by either AChE inhibition or other mechanisms. There are some observations indicating that not all the effects of OP insecticides are due to AChE inhibition. For example, acetylcholine esterase knockout mice exhibit symptoms of neurotoxicity induced by exposure to OP insecticides (Duysen et al., 2001). Moreover, the toxicity of OP insecticides, particularly in response to chronic OP exposure, occurs in the absence of ChE inhibition (Banks and Lein, 2012). In this study, we examined the effects of diazinon in macrophages under *in vitro* or *ex vivo* conditions. Since acetylcholine could not be induced under our experimental conditions, macrophage activation induced by diazinon could have been mediated by a mechanism other than inhibition of AChE.

Since diazinon is sprayed on agricultural crops before harvest, diazinon could be absorbed by inhalation route, and the local concentration of diazinon could be high in the airway and lung where macrophages are abundant. We used 150-600 μM diazinon to maintain diazinon at high local concentrations and mimic a physiologically relevant *in vivo* exposure by diazinon.

We first demonstrated that diazinon significantly enhanced the mRNA expression and protein production of proinflammatory cytokines such as TNF-α and IL-6 in RAW264.7 cells. We also demonstrated that diazinon induced TNF-α and IL-6 in BALF cells, which predominantly contain alveolar macrophages. These observations

led us to examine whether exposure to diazinon could activate macrophages and further enhance proinflammatory responses. We next examined the expression of COX-2 and iNOS in RAW264.7 cells. COX-2 expression is highly restricted under basal conditions and up-regulated during inflammation in various cell types (Tilley et al., 2001). Diazinon significantly increased the expression of COX-2 and iNOS. These results also suggested that exposure to diazinon could enhance the proinflammatory response induced by macrophages.

Macrophages act as professional antigen presenting cells and can prime T cells through the up-regulation of MHC class II molecules and costimulatory molecules, such as CD40, CD80, and CD86. In this study, we showed that diazinon up-regulated the expressions of CD40, CD86, and MHC class II in RAW264.7 cells, suggesting that it can potentially provide an antigen-presenting phenotype for macrophages.

Phagocytic activity is one of the physiological functions of macrophages that signals the beginning of the immune response and, in turn orchestrates the adaptive immune response. Although diazinon induced the expression of proinflammatory cytokines, COX-2, iNOS, and cell-surface molecules, which suggested the activation of macrophages, phagocytic activity was decreased by diazinon in RAW264.7 cells. It has been reported that dendritic cells downregulate antigen internalization and increase the surface expression of costimulatory molecules when converted from immature to mature cells (Banchereau et al., 2000). Since macrophages are also antigen presenting cells as well as dendritic cells, macrophages might be activated at different phases for phagocytosis and the upregulation of costimulatory molecules. Moreover, it may also be partially explained by the significant induction of COX-2. PGE_2, which is produced by COX-2, is a potent mediator of inflammation that induces both pro- and anti-inflammatory effects (Medeiros et al., 2012). Recent studies have demonstrated that PGE_2 can inhibit phagocytosis through the E prostanoid (EP) 2 receptor by increasing

cAMP levels (Aronoff et al., 2004; Canetti et al., 2007). RAW264.7 cells have been reported to express EP2 receptor (Tajima et al., 2008), and its expression could be regulated in a manner that is dependent on inflammatory stimuli (Hubbard et al., 2001). Thus, suppression of phagocytic activity by diazinon in RAW264.7 cells was likely due at least in part to the increase of PGE_2 production induced by COX-2.

Insecticide-induced oxidative stress as a possible mechanism of toxicity has been reported (Altuntas et al., 2004; Milatovic et al., 2006). In this study, we showed that diazinon elevated intracellular ROS generation in RAW264.7 cells. In normal circumstances, ROS generation is balanced by the presence of antioxidant enzymes such as HO-1, glutathione peroxidase, superoxide dismutase, and catalase. The induction of HO-1 expression confirmed that diazinon generated excess ROS and caused oxidative stress in macrophages. Since diazinon has been reported to change the activities of anti-oxidant enzymes, exposure to diazinon could cause much more severe damage to macrophages (Altuntas et al., 2004). Moreover, recent reports have suggested that ROS can act as signaling molecules to trigger proinflammatory cytokine production and the expressions of iNOS and COX-2 by inflammatory stimuli such as LPS (Nakahira et al., 2011; Tsai et al., 2013; Zhou et al., 2011), suggesting that overproduction of ROS by diazinon might initiate macrophage activation.

One of the most important pathways activated by ROS involves NF-κB. NF-κB is a main transcription factor involved in the transcription of various inflammatory molecules induced by macrophages, including inflammatory cytokines, iNOS, and COX-2. Interestingly, diazinon did not alter the phosphorylation of p65, suggesting that another transcription factor might be involved in diazinon-induced TNF-α, IL-6, iNOS, and COX-2 expression. We also determined that diazinon induced phosphorylation of ERK and p38, but not JNK. Moreover, diazinon-induced IL-6 induction was mediated by both ERK and p38, suggesting that ERK- and p38-dependent

transcription factors might be involved in diazinon-mediated induction of various inflammatory molecules in macrophages. Since various transcription factors as well as NF-κB can be activated by ROS, it has been reported that ROS-mediated ERK and p38 phosphorylation would activate CREB, leading to IL-6 gene expression (Sano et al., 2001). Moreover, CREB inhibits NF-κB activation even though CREB positively regulates the expression of TNF-α, IL-6, and COX-2 (Wen et al., 2010; Sano et al., 2001). These observations suggested that activation of CREB might be involved in diazinon-mediated induction of various inflammatory molecules in macrophages.

This study clearly demonstrated that diazinon could activate macrophages and enhance inflammatory responses. Caution should thus be taken to avoid direct exposure to diazinon via dermal and inhalation pathways. Further studies are warranted to better characterize the mechanisms that cause immunomodification by diazinon.

References

Ahmed, M.A., Ahmed, H.I. El-Morsy, E.M., 2013. Melatonin protects against diazinon-induced neurobehavioral changes in rats. Neurochem. Res. 38, 2227-2236.

Altuntas, I., Kilinc, I., Orhan, H., Demirel, R., Koylu, H., Delibas, N., 2004. The effects of diazinon on lipid peroxidation and antioxidant enzymes in erythrocytes in vitro. Hum. Exp. Toxicol. 23, 9-13.

Aronoff, D.M., Canetti, C., Peters-Golden, M., 2004. Prostaglandin E2 inhibits alveolar macrophage phagocytosis through an E-prostanoid 2 receptor-mediated increase in intracellular cyclic AMP. J. Immunol. 173, 559-565.

Banchereau, J., Briere, F., Caux, C., Davoust, J., Lebecque, S., Liu, Y.J., Pulendran, B., Palucka, K., 2000. Immunobiology of dendritic cells. Annu. Rev. Immunol. 18, 767-811.

Banerjee, I., Tripathi, S., Roy, A.S., 2012. Clinico-epidemiological characteristics of patients presenting with organophosphorus poisoning. N. Am. J. Med. Sci. 4, 147-150.

Banks, C.N., Lein, P.J., 2012. A review of experimental evidence linking neurotoxic organophosphorus compounds and inflammation. Neurotoxicology 33, 575-584.

Canetti, C., Serezani, C.H., Atrasz, R.G., White, E.S., Aronoff, D.M., Peters-Golden, M., 2007. Activation of phosphatase and tensin homolog on chromosome 10 mediates the inhibition of FcgammaR phagocytosis by prostaglandin E2 in alveolar macrophages. J. Immunol. 179, 8350-8356.

Duysen, E.G., Li, B., Xie, W., Schopfer, L.M., Anderson, R.S., Broomfield, C.A., Lockridge, O., 2001. Evidence for nonacetylcholinesterase targets of organophosphorus nerve agent: supersensitivity of acetylcholinesterase knockout mouse to VX lethality. J. Pharmacol. Exp. Ther. 299, 528-535.

Flaskos, J., 2012. The developmental neurotoxicity of organophosphorus insecticides: a direct role for the oxon metabolites. Toxicol. Lett. 209, 86-93.

Gordon, S., 2003. Alternative activation of macrophages. Nat. Rev. Immunol. 3, 23-35.

Handy, R.D., Abd-El Samei, H.A., Bayomy, M.F., Mahran, A.M., Abdeen, A.M., El-Elaimy, E.A., 2002. Chronic diazinon exposure: pathologies of spleen, thymus, blood cells, and lymph nodes are modulated by dietary protein or lipid in the mouse. Toxicology 172, 13-34.

Hariri, A.T., Moallem, S.A., Mahmoudi, M., Memar, B., Hosseinzadeh, H., 2010. Sub-acute effects of diazinon on biochemical indices and specific biomarkers in rats: protective effects of crocin and safranal. Food Chem. Toxicol. 48, 2803-2808.

Hubbard, N.E., Lee, S., Lim, D., Erickson, K.L., 2001. Differential mRNA expression of prostaglandin receptor subtypes in macrophage activation. Prostaglandins Leukot. Essent. Fatty Acids 65, 287-294.

Lein, P.J., Fryer, A.D., 2005. Organophosphorus insecticides induce airway hyperreactivity by decreasing neuronal M2 muscarinic receptor function independent of acetylcholinesterase inhibition. Toxicol. Sci. 83, 166-176.

Medeiros, A., Peres-Buzalaf, C., Fortino Verdan, F., Serezani, C.H., 2012. Prostaglandin E2 and the suppression of phagocyte innate immune responses in different organs. Mediators Inflamm. 2012, 327568.

Milatovic, D., Gupta, R.C., Aschner, M., 2006. Anticholinesterase toxicity and oxidative stress. Sci. World J. 6, 295-310.

Nakahira, K., Haspel, J.A., Rathinam, V.A., Lee, S.J., Dolinay, T., Lam, H.C., Englert, J.A., Rabinovitch, M., Cernadas, M., Kim, H.P., Fitzgerald, K.A., Ryter, S.W., Choi, A.M., 2011. Autophagy proteins regulate innate immune responses by inhibiting the release of mitochondrial DNA mediated by the NALP3 inflammasome. Nat. Immunol. 12, 222-230.

Pizzurro, D.M., Dao, K., Costa, L.G., 2014. Diazinon and diazoxon impair the ability of astrocytes to foster neurite outgrowth in primary hippocampal neurons. Toxicol. Appl.

Pharmacol. 274, 372-382.

Proskocil, B.J., Bruun, D.A., Jacoby, D.B., van Rooijen, N., Lein, P.J., Fryer, A.D., 2013. Macrophage TNF-alpha mediates parathion-induced airway hyperreactivity in guinea pigs. Am. J. Physiol. Lung Cell. Mol. Physiol. 304, L519-529.

Sano, M., Fukuda, K., Sato, T., Kawaguchi, H., Suematsu, M., Matsuda, S., Koyasu, S., Matsui, H., Yamauchi-Takihara, K., Harada, M., Saito, Y., Ogawa, S., 2001. ERK and p38 MAPK, but not NF-kappaB, are critically involved in reactive oxygen species-mediated induction of IL-6 by angiotensin II in cardiac fibroblasts. Circ. Res. 89, 661-669.

Shibasaki, M., Hashimoto, K., Okamoto, M., Hayashi, Y., Imaizumi, K., Hashimoto, N., Ozaki, N., Yokoi, T., Takagi, K., Hasegawa, Y., Shimokata, K., Kawabe, T. 2009. Up-regulation of surfactant protein production in a mouse model of secondary pulmonary alveolar proteinosis. Am. J. Respir. Cell Mol. Biol. 40, 536-542.

Tajima, T., Murata, T., Aritake, K., Urade, Y., Hirai, H., Nakamura, M., Ozaki, H., Hori, M., 2008. Lipopolysaccharide induces macrophage migration via prostaglandin D(2) and prostaglandin E(2). J. Pharmacol. Exp. Ther. 326, 493-501.

Takashima, K., Matsushima, M., Hashimoto, K., Nose, H., Sato, M., Hashimoto, N., Hasegawa, Y., Kawabe, T., 2014. Protective effects of intratracheally administered quercetin on lipopolysaccharide-induced acute lung injury. Respir. Res. 15, 150.

Terry Jr., A.V., 2012. Functional consequences of repeated organophosphate exposure: potential non-cholinergic mechanisms. Pharmacol. Ther. 134, 355-365.

Tilley, S.L., Coffman, T.M., Koller, B.H., 2001. Mixed messages: modulation of inflammation and immune responses by prostaglandins and thromboxanes. J. Clin. Invest. 108, 15-23.

Tsai, H.H., Lee, W.R., Wang, P.H., Cheng, K.T., Chen, Y.C., Shen, S.C., 2013. Propionibacterium acnes-induced iNOS and COX-2 protein expression via ROS-

dependent NF-kappaB and AP-1 activation in macrophages. J. Dermatol. Sci. 69, 122-131.

Wen, A.Y., Sakamoto, K.M., Miller, L.S., 2010. The role of the transcription factor CREB in immune function. J. Immunol. 185, 6413-6419.

Win-Shwe, T.T., Nakajima, D., Ahmed, S., Fujimaki, H., 2013. Impairment of novel object recognition in adulthood after neonatal exposure to diazinon. Arch. Toxicol. 87, 753-762.

Yasui, M., Matsushima, M., Omura, A., Mori, K., Ogasawara, N., Kodera, Y., Shiga, M., Ito, K., Kojima, S., Kawabe, T., 2015. The suppressive effect of quercetin on toll-like receptor 7-mediated activation in alveolar macrophages. Pharmacology 96, 201-209.

Zhou, R., Yazdi, A.S., Menu, P., Tschopp, J., 2011. A role for mitochondria in NLRP3 inflammasome activation. Nature 469, 221-225.

Figure legends

Figure 1. Effects of diazinon on cell viability and the production of proinflammatory cytokines in RAW264.7 cells.

(A) RAW264.7 cells were exposed to a series of concentrations of diazinon (50-600 μM) or vehicle (DMSO) for 24 h. At the end of the incubation, WST-1 reagent was added and incubated for 1 h. Values are expressed as means ± SD of triplicates from a representative of three independent experiments.

(B) RAW264.7 cells were incubated with diazinon (600 μM) or vehicle (DMSO) for 1 h (TNF-α) or 4 h (IL-6), and the expression levels of TNF-α- and IL-6-encoding transcripts were determined by quantitative real-time PCR.

(C) RAW264.7 cells were incubated with diazinon (600 μM) or vehicle (DMSO) for 24 h, and the production of TNF-α and IL-6 in the supernatant of culture medium after stimulation of diazinon was determined. Values are expressed as means ± SD of triplicates from a representative of three independent experiments. Asterisks indicate significant differences from control cells ($p<0.05$).

Figure 2. Effects on ROS generation and HO-1, COX-2, and iNOS expression induced by diazinon in RAW264.7 cells.

(A) RAW264.7 cells were loaded with 50 μM H_2DCF-DA for 15 min, subsequently incubated with diazinon (150, 300, 600 μM), H_2O_2 (600 μM), or vehicle (DMSO) for 15 min, and intracellular ROS was measured by a flow cytometer. Representative result from three independent experiments was shown, and intracellular ROS generation were quantified as mean fluorescence intensity (MFI).

(B-D) RAW264.7 cells were incubated with diazinon (600 μM) or vehicle (DMSO) for 4 h, and the expression levels of HO-1- (B), COX-2- (C), and iNOS- (D)-encoding transcripts were determined by quantitative real-time PCR. Results are expressed as

means ± SD of triplicates from a representative of three independent experiments. Asterisks indicate significant difference from control cells ($p<0.05$).

Figure 3. Effects of diazinon on the expression of cell-surface molecules in RAW264.7 cells.

RAW264.7 cells were incubated with 600 μM diazinon or vehicle (DMSO) for 25 h, and the expressions of cell-surface molecules (CD40, CD80, CD86, and MHC class II) after stimulation of diazinon were shown. The shaded histogram represents unstained cells. Representative result from more than three independent experiments was shown, and the expression levels of cell-surface molecules were quantified as MFI.

Figure 4. Effects of diazinon on phagocytosis in RAW264.7 cells.

RAW264.7 cells were incubated with diazinon (150, 600 μM) or vehicle (DMSO) for 20 h, and phagocytic internalization of FITC-labeled latex beads by RAW264.7 cells was evaluated. Representative result from more than three independent experiments was shown, and the levels of phagocytosis were quantified as MFI.

Figure 5. Effects of diazinon on phosphorylation of NF-κB and MAP kinase.

(A) RAW264.7 cells were incubated with diazinon (600 μM), LPS (10 μg/ml) + IFN-γ (100 ng/ml), or vehicle (DMSO) for 20 min. The phosphorylations of p65, ERK, p38, and JNK were determined by western blotting. Representative result from three independent experiments was shown, the ratio of p-p65/p65, p-ERK/ERK, p-p38/p38, and p-JNK/JNK was quantified by using Scion Image software.

(B) RAW264.7 cells were pretreated with either PD98059 (30 μM) or SB202190 (15 μM) for 1 h and then incubated with diazinon (600 μM) or vehicle (DMSO) for another 4 h. The expression levels of IL-6-encoding transcripts were determined by

quantitative real-time PCR. Values are expressed as means ± SD of triplicates from a representative of three independent experiments. Asterisks indicate significant differences from cells treated with diazinon ($p<0.05$).

Figure 6. Effects of diazinon on the expression of cell-surface molecules and phagocytosis in BMDM.

(A) BMDM were incubated with 300 μM diazinon or vehicle (DMSO) for 25 h, and the expressions of cell-surface molecules (CD40, CD80, CD86, and MHC class II) on CD11b-gated cells after stimulation of diazinon were shown. The shaded histogram represents unstained cells. Representative result from three independent experiments was shown, and the expression levels of cell-surface molecules were quantified as MFI.

(B) BMDM were incubated with 300 μM diazinon or vehicle (DMSO) for 20 h, and phagocytic internalization of FITC-labeled latex beads by CD11b-gated cells was evaluated. Representative result from three independent experiments was shown, and the levels of phagocytosis were quantified as MFI.

Figure 7. Effects of diazinon on cytokine expression in mouse BALF cells.

Mouse BALF cells were stimulated with 150 μM diazinon for 4 h. The expression levels of TNF-α- and IL-6-encoding transcripts were determined by quantitative real-time PCR. Results are expressed as means ± SD of triplicates from a representative of three independent experiments. Asterisks indicate significant differences ($p<0.05$).

Figure 1

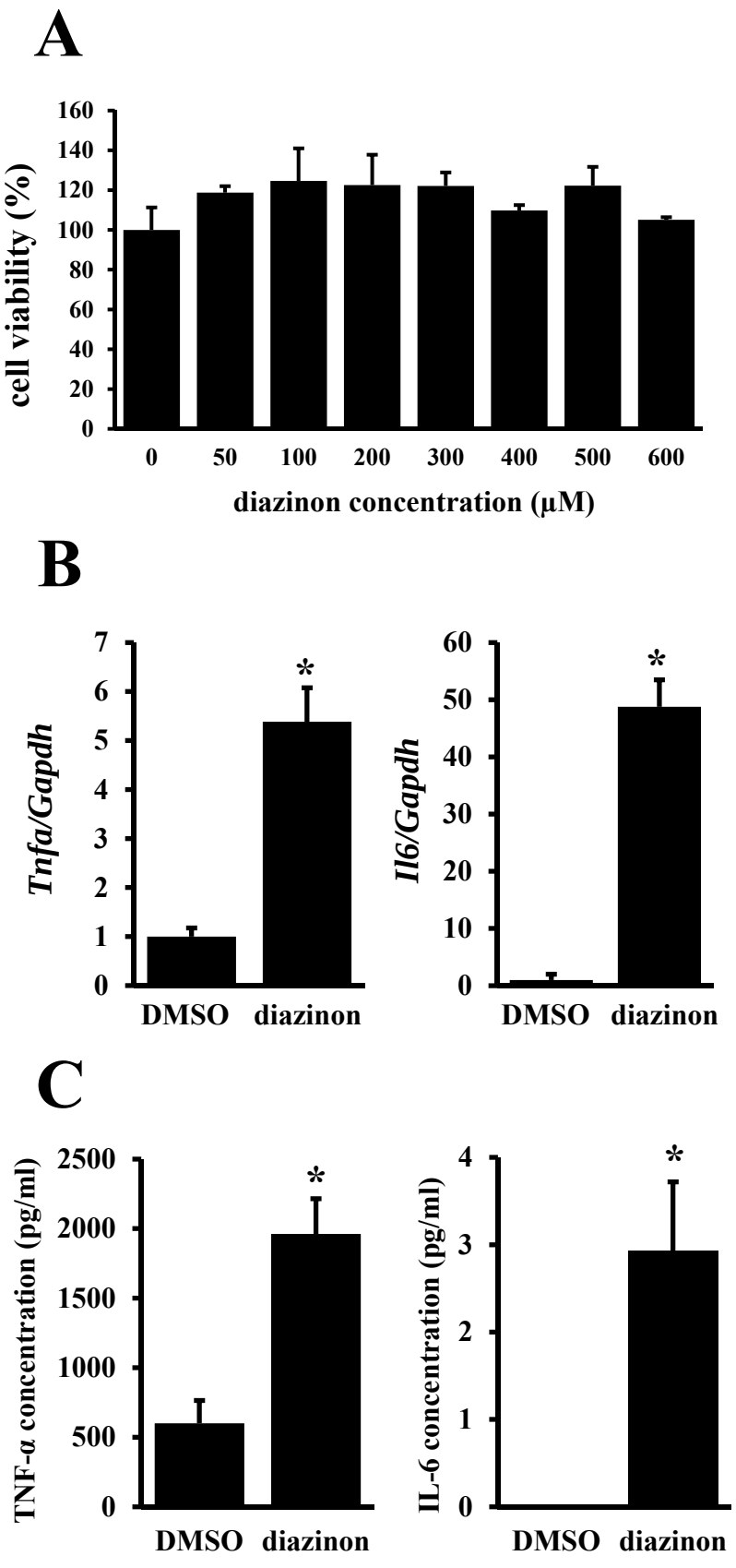
A
cell viability (%)
160
140
120
100
80
60
40
20
0
0
50
100
200
300
400
500
600
diazinon concentration (μM)
B
Tnfa/Gapdh
7
6
5
4
3
2
1
0
*
DMSO
diazinon
Il6/Gapdh
60
50
40
30
20
10
0
*
DMSO
diazinon
C
TNF-α concentration (pg/ml)
2500
2000
1500
1000
500
0
*
DMSO
diazinon
IL-6 concentration (pg/ml)
4
3
2
1
0
*
DMSO
diazinon

Figure 2

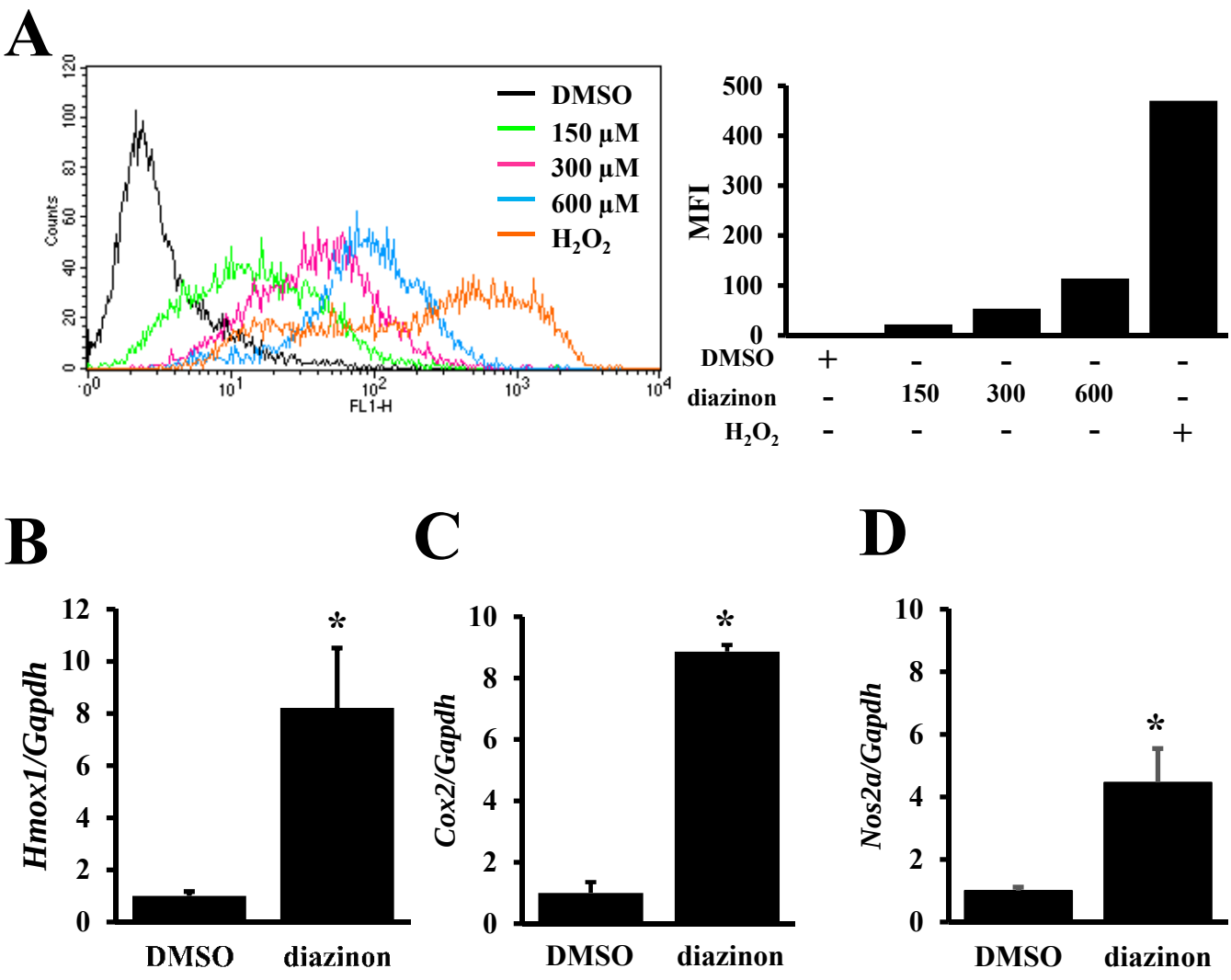
A
DMSO
150 μM
300 μM
600 μM
H2O2
Counts
FL1-H
MFI
DMSO
diazinon
H2O2
B
Hmox1/Gapdh
C
Cox2/Gapdh
D
Nos2a/Gapdh
DMSO
diazinon

Figure 3

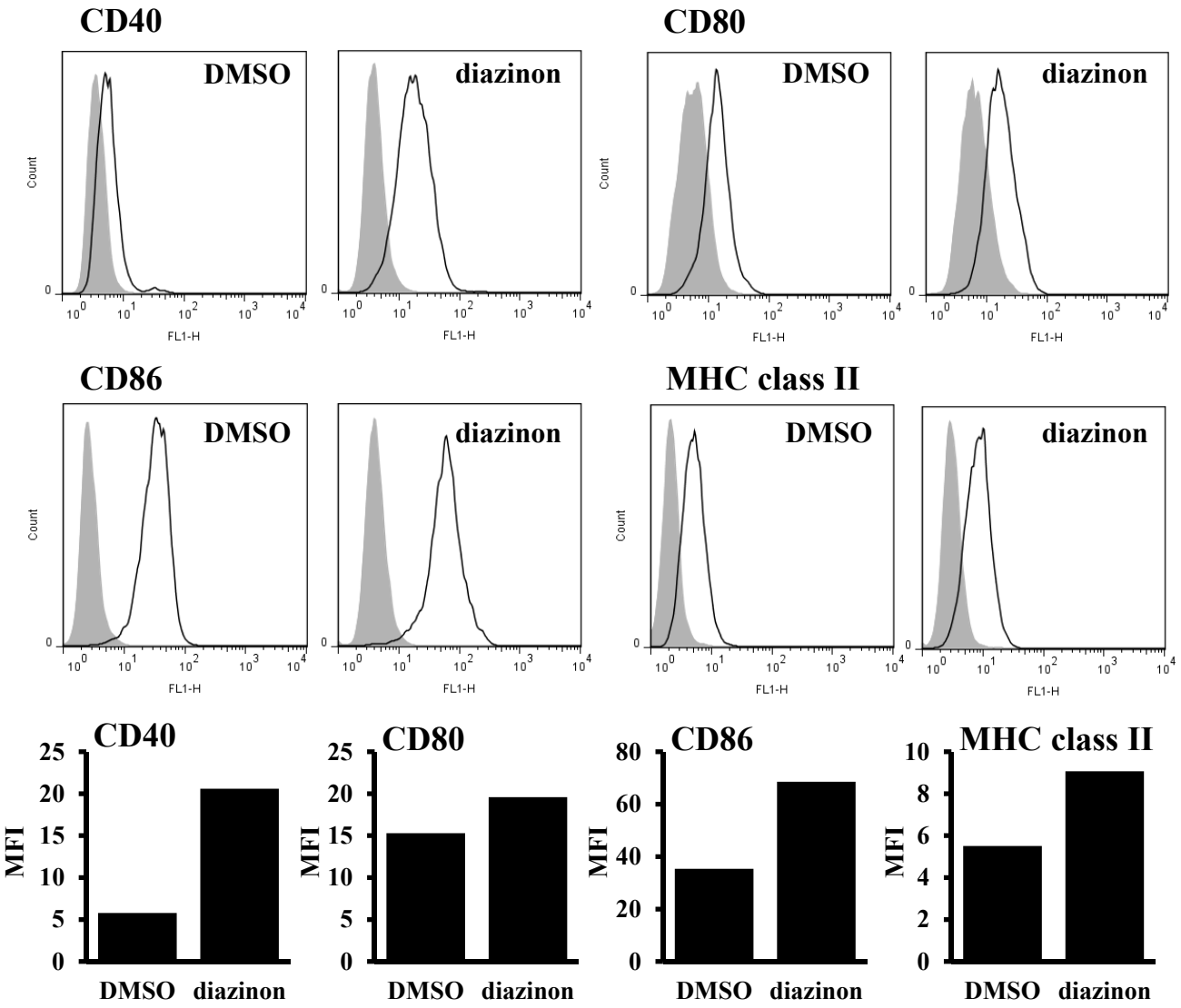
CD40
DMSO
diazinon
CD80
DMSO
diazinon
CD86
DMSO
diazinon
MHC class II
DMSO
diazinon
Count
FL1-H
CD40
CD80
CD86
MHC class II
MFI
DMSO
diazinon

Figure 4

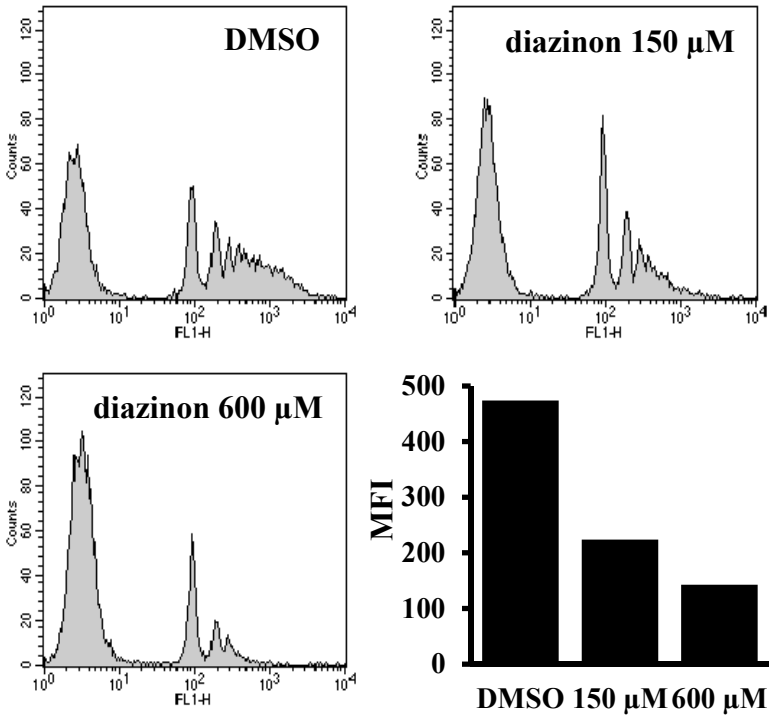
DMSO
diazinon 150 µM
diazinon 600 µM
Counts
FL1-H
MFI
500
400
300
200
100
0
DMSO
150 µM
600 µM

Figure 5

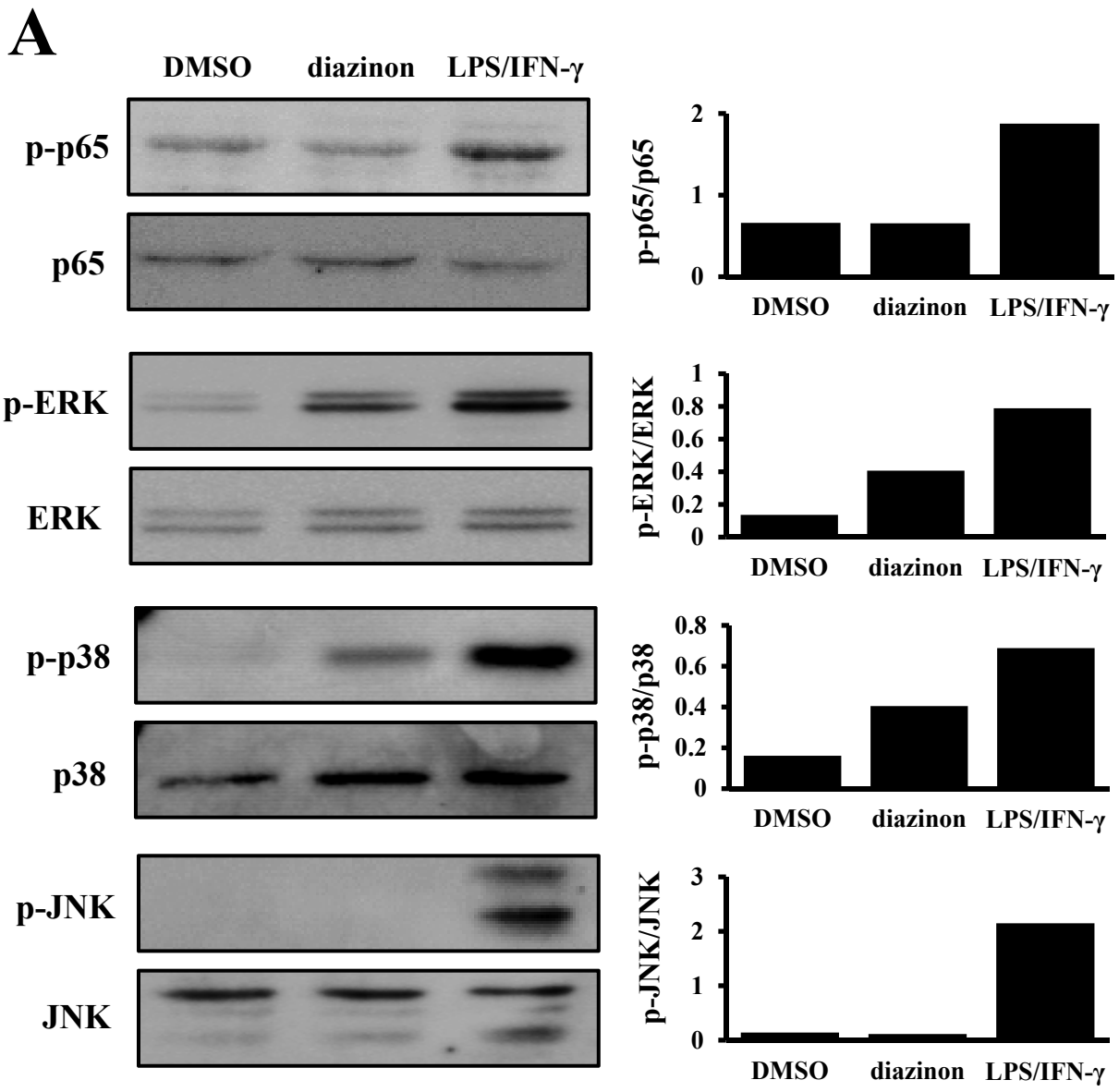
A
DMSO
diazinon
LPS/IFN-γ
p-p65
p65
p-ERK
ERK
p-p38
p38
p-JNK
JNK
p-p65/p65
p-ERK/ERK
p-p38/p38
p-JNK/JNK
B
Il6/Gapdh
80
60
40
20
0
*
*
DMSO + - - - - -
diazinon - + + + - -
PD98059 - - + - + -
SB202190 - - - + - +

Figure 6

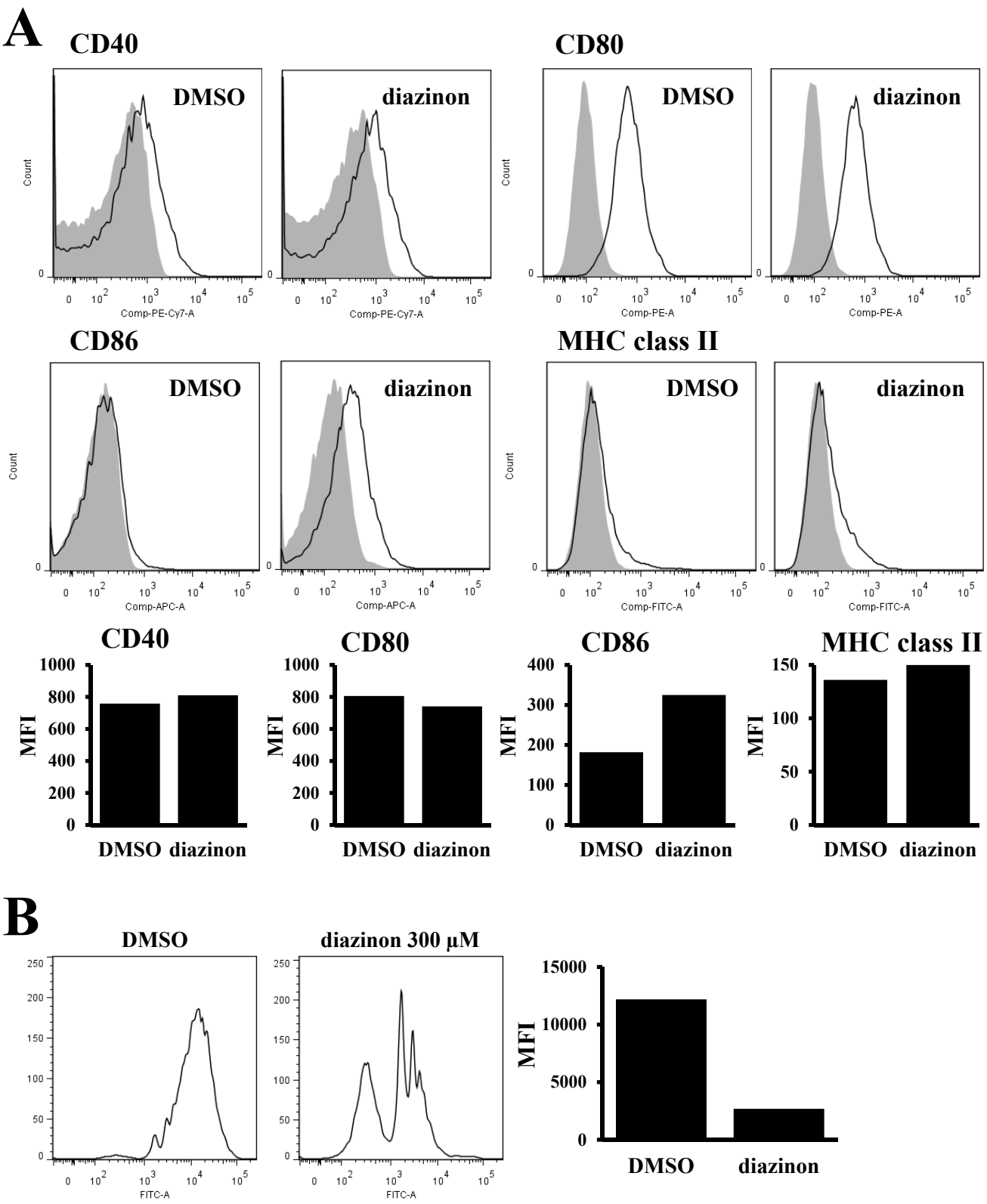
A
CD40
DMSO
diazinon
Count
Comp-PE-Cy7-A
CD80
Comp-PE-A
CD86
Comp-APC-A
MHC class II
Comp-FITC-A
MFI
DMSO diazinon
B
DMSO
diazinon 300 µM
FITC-A

Figure 7

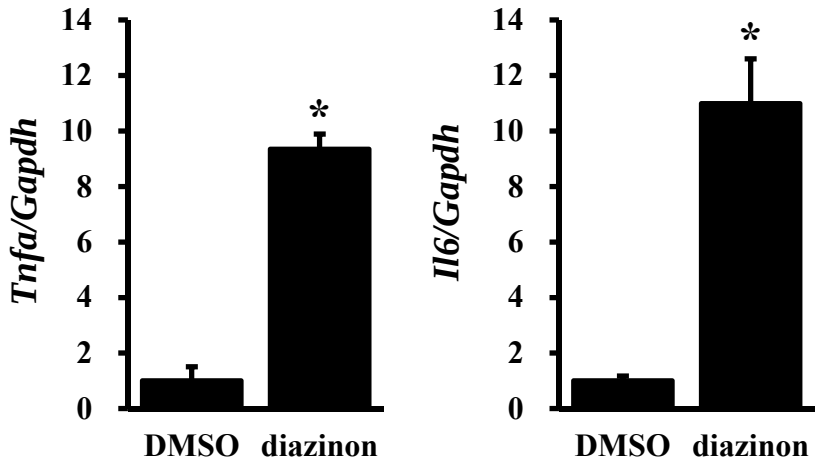
Tnfa/Gapdh
14
12
10
8
6
4
2
0
*
DMSO
diazinon
Il6/Gapdh
14
12
10
8
6
4
2
0
*
DMSO
diazinon